Kinetics, Thermodynamics and Structure: An Analysis of Corn Starch Acetylation

Roberta Ranielle Matos de Freitas[a,b] [ID], *Karina Palmizani do Carmo[2]* [ID],

Franciane Andrade de Pádua[a] [ID]*, Vagner Roberto Botaro[a,b]* [ID]

[a]*Universidade Federal de São Carlos, Programa de Pós-Graduação em Planejamento e Uso de Recursos Renováveis, Sorocaba, SP, Brasil.*
[b]*Universidade Federal de Ouro Preto, Programa de Pós-Graduação em Engenharia de Materiais, Ouro Preto, MG, Brasil.*

This study investigated the kinetics and thermodynamics of starch acetylation and examined the influence of the degree of substitution (DS) on the properties of acetylated starches. Starch acetylation kinetics followed a pseudo-first-order model, reaching a degree of substitution of 2.62 after 50 minutes. Negative enthalpy and entropy values revealed a non-spontaneous reaction requiring catalysis. Fourier Transform Infrared Spectroscopy confirmed acetylation through the appearance of a carbonyl band and the reduction of the glycosidic bond peak. Increasing degree of substitution caused granule breakage, agglutination, and reduced crystallinity, as evidenced by Scanning Electron Microscopy and X-Ray Diffraction. Dynamic Mechanical Analysis demonstrated that these structural changes reduced the glass transition in high degrees of substitution (DS 2.62) and enhanced thermal stability and viscoelastic properties due to the loss of crystallinity. Understanding these processes facilitates the industrial optimization of starch acetylation, resulting in modified starches with improved properties for diverse applications.

Keywords: *Acetylation, corn starch, kinetic study, reaction thermodynamics, SEM, FTIR.*

1. Introduction

Starch is a naturally occurring polysaccharide found in various plants, where it serves as a crucial energy reserve. Its unique properties make it a versatile raw material widely used across industries, including food, pharmaceuticals, and textiles[1]. However, the highly hydrophilic nature of native starch limits its functionality in certain industrial processes. To overcome this limitation, chemical modifications such as acetylation are commonly applied to enhance the physicochemical properties of starch, thereby expanding its potential applications[2].

In acetylation, hydroxyl groups in starch molecules are replaced with acetyl groups through an esterification reaction, producing starch acetate (SA)[3]. The Degree of Substitution (DS) indicates the average number of substituted hydroxyl groups per glucose unit, ranging from zero to three[4]. DS is an essential parameter, as it directly influences the functional properties of acetylated starch[5], such as hydrophobicity, thermal stability, and moisture resistance[6]. Starch acetate with varying DS values is used in diverse fields[7], including film coatings[4], controlled-release drug formulations[8,9], and textile adhesives[9].

Betancur et al.[10] reported that acetylation enhances the functional properties of Jack bean starch, making it suitable for industrial applications like food thickening and stabilization. Subsequent research has explored various starch sources and acetylation methods, including the acetylation of potato starch under catalysis by different hydroxides[11]; acetylation of corn starch under Ultrahigh Pressure (UHP)[12]; corn starch acetylated with acetic anhydride and iodine[10]; and acetylated using sodium hydroxide and acetic anhydride[13,14]. These studies emphasize that the acetylation process can significantly alter the structural, thermal, and mechanical properties of starch, thereby improving its suitability for industrial applications.

The kinetics and thermodynamics of starch acetylation are essential for optimizing the process; however, few studies have thoroughly examined these aspects. While previous research suggests that the reaction follows pseudo-first-order kinetics[15], influenced by factors such as time, temperature, and catalysts, the majority of the literature focuses on reaction efficiency and the properties of modified starch[16-18]. This lack of detailed analysis of the kinetic and thermodynamic parameters under varying conditions limits a comprehensive understanding and optimization of the process for large-scale applications.

This study aims to investigate the kinetics and thermodynamics of the starch acetylation reaction. By analyzing the influence of the (DS) on the properties of acetylated starches, we seek to provide a more complete understanding of the acetylation process. Additionally, the study utilizes Scanning Electron Microscopy (SEM) to examine morphological changes, Fourier Transform Infrared Spectroscopy (FTIR) to confirm

*e-mail: roberta.ranielle@hotmail.com

the presence of acetyl groups, X-ray Diffraction (XRD) to assess changes in crystalline structure, and Dynamic Mechanical Analysis (DMA) to evaluate the mechanical properties of the modified starch. The results of this research will help optimize starch acetylation for various industrial applications, enhancing the functional and structural properties of starch-based materials.

2. Materials and Methods

2.1. Starch acetylation

The corn starch used was AMILOGILL® 2100 (CAS - Chemical Abstracts Service Number: 9005-25-8) contains 25% amylose and 75% amylopectin, as indicated by the supplied by the company Cargill®. Starch acetylation was performed according to the procedure used by Larotonda et al.[4], based on patent (US Patent No. 5,710,269) by Bernice L. Feuer, filed by Hoescht Celanes and Corp., Somerville, New Jersey. In a 1000mL beaker, 75 g of dry starch, 135 mL of glacial acetic acid P.A. and 138 mL of acetic anhydride P.A. were mixed and stirred for 30 minutes without heating. Afterward, a catalyst mixture (1.05 mL of concentrated sulfuric acid and 12.45 mL of glacial acetic acid) was carefully added. Samples were collected at fixed intervals of 10 min, up to 160 min; then, they were precipitated in water at 10 °C. To thoroughly remove solvent and reagent residues from the acetylated starch samples, the washing process was repeated several times using an excess of deionized water until the wash water reached a neutral pH. This step was crucial to minimize contamination by residual reagents and ensure the purity of the final acetylated starch product. The washed samples were subsequently vacuum-filtered and dried in an oven at 50 °C for 24 hours.

2.2. Determination of DS

The DS was determined by hydrating 1.0 g of starch acetate in 50 mL of an alcoholic solution (P.A. 75% v/v absolute ethyl alcohol) and heating it at 50 °C for 30 min. After cooling, 30 mL of sodium hydroxide (0.5 N) was added to this solution, which was then stirred for 72 hours at room temperature. Phenolphthalein was added as an indicator, and the excess alkali was titrated with 0.5 mol/L hydrochloric acid[4]. A reference sample was analyzed using the same method. The percentage of acetylation was calculated using Equation 1:

$$\%A = \frac{\left[(Vo-Vn)\,xNx0.043x100\right]}{M} \tag{1}$$

Vo = volume of HCl (0.5 N) used to titrate reference sample; Vn = volume of HCl (0.5 N) used to titrate acetate sample; N = HCl used normality; 43 = molar mass of acetyl group (g/mol); M = mass of weighted sample (g). The DS was calculated using the percentage of acetylation through Equation 2:

$$DS = \frac{\left[162x\%A\right]}{\left[4300-(42x\%A)\right]} \tag{2}$$

2.3. Fourier Transform Infrared Spectroscopy (FTIR)

Samples were characterized using FTIR (Perkin Elmer - Spectrum 65 FT-IR USA) to identify the main bands and their variations, including reduction, narrowing and widening. Analyzes were performed using ATR method with a scan of 4000 to 400 cm⁻¹, spectral resolution. 0.5 cm⁻¹ and 32 scans.

2.4. Starch acetylation kinetics and thermodynamics

Kinetics analyses were performed to determine the reaction order and constant k, based on data collected from the start of the reaction until the maximum acetylation time (from 10 to 40 min), where the direct reaction was complete. The rate law was studied based on hydroxyl group consumption along the starch chain, and Equation 3 was used to calculate OH consumption as a percentage for each DS obtained.

$$\%OHconsumption = 100 - \left[\left(\frac{DS}{3}\right)\times100\right] \tag{3}$$

In kinetic studies of higher-order reactions, conditions were often used in which these reactions exhibited a kinetic behavior of "apparently" first, second, or even zero order, referred to as pseudo-order. This condition was applied when one of the reagents was in excess, making it constant in the rate equation. Consequently, the following equations were employed for pseudo-first order (Equation 4), second order (Equation 5), and zero order (Equation 6):

$$ln\left[\%OH\right]_t = ln\left[\%OH\right]_0 - k_1 t \tag{4}$$

$$\frac{1}{\left[\%OH\right]} = kt + \frac{1}{\left[\%OH\right]_0} \tag{5}$$

$$\left[\%OH\right] = -kt + \left[\%OH\right]_0 \tag{6}$$

Where %OH = amount in percentage of OH consumed with reaction, t = time and k = constant[19].

To calculate the thermodynamic parameters, the following equations were used:

$$ln\theta_T = \frac{-\Delta H}{RT} + \frac{\Delta H}{RT_0} + ln\theta_0 \tag{7}$$

$$\Delta H = \int_{T_1}^{T_2} C_p dT = C_p(T_2 - T_1) \tag{8}$$

$$\Delta S = C_p ln\left(\frac{T_2}{T_1}\right) \tag{9}$$

where ΔH = heat of starch acetylation, T_0 = critical temperature of acetylation, T = temperature, R = universal gas constant, C_p = heat capacity, θ_0 = critical degree of starch acetylation, and ΔS =.entropy variation value[19].

2.5. Scanning Electron Microscopy (SEM)

SEM was used to analyze morphological changes caused by acetylation. Samples were examined using a Hitachi TM 3000 model, with an acceleration of 5 Kv and an magnifications of 300x, 1000x and 4000x. For preparation, powdered samples were dried in an oven at 60 °C for 24 hours and stored in a desiccator. Analyses were performed without metallic coating.

2.6. X-ray Diffraction (XRD)

XRD analyses were performed using the SHIMADZU-JP X-ray diffractometer (model XRD-6100), consisting of the main unit, X-ray tube A-45-Cu, SC-1001 scintillation detector for XRD-6100, and CM-3121 monochromator for a copper target. Powdered samples (starch and starch acetates with varying DS) were exposed to CuKα radiation at 30 mA, 40 kV, with a scanning speed of $2\Theta = 1°/min$ in the range of 3 - 40°. The crystallinity index (Xc) was calculated using the peak deconvolution method, which was performed with computer programs that employed profile functions such as Gaussian, Lorentzian, and Voigt to fit the curves resulting from the crystalline contributions of each peak and the non-crystalline contribution of the sample. The pseudo-Voigt Function type 1 was applied in the software Origin (version 8.5, Microcal Inc., Northampton, MA, USA). The crystallinity index (Xc) was determined as the ratio of the area of the crystalline peaks to the total area of the diffractogram.

2.7. Dynamic Mechanical Analysis (DMA)

DMA was conducted using a Q800 (TA Instruments) with a custom-designed powder sample holder. The holder was specifically created to maintain the powder in a defined geometry. It consisted of an open, rectangular stainless steel container with internal dimensions of 60 mm x 11.5 mm x 1 mm, along with a lid (Figure 1a). Approximately 0.2 g of powdered starch and starch acetate samples were evenly distributed within the shallow container, and the top plate (lid) was placed on the powder's surface. The lid was designed to fit precisely within the container's walls (Figure 1b). The sample holder, containing the powder, was then placed into the dual cantilever clamp (Figure 1c) and secured at three points with a fixed pressure of 5 psi, ensuring uniform pressure exerted on the lid and the powder inside the holder. The analyses were conducted with a heating rate of 3 °C/min, spanning from -50 to 180 °C, an amplitude of 20 μm, and a fixed frequency of 1 Hz[20].

3. Results and Discussion

3.1. Starch acetylation

Figure 2 illustrates the results obtained for corn starch acetylation as a function of time and temperature. The DS reached a maximum value of 2.6 at approximately 50 minutes, after which the reaction stabilized, indicating equilibrium. Temperature fluctuations were recorded during the process. Although no external heat was applied, the catalyst increased the temperature from 19 °C to 50 °C, suggesting the reaction was exothermic.

This temperature increase likely resulted from an exothermic reaction mechanism, primarily the dehydration of starch in the presence of acetic acid. This dehydration was crucial for facilitating the acetylation process, as it removed water molecules that could otherwise hinder the formation of acetyl bonds by hydrolyzing acetic anhydride. Additionally, residual moisture in the starch may have reacted with acetic anhydride through hydrolysis, releasing heat and contributing further to the temperature rise[21]. The catalyst likely played a role in heat generation by lowering the activation energy and accelerating the exothermic reactions. Consequently, this exothermic behavior enhanced the efficiency of the reaction by promoting the substitution of hydroxyl groups
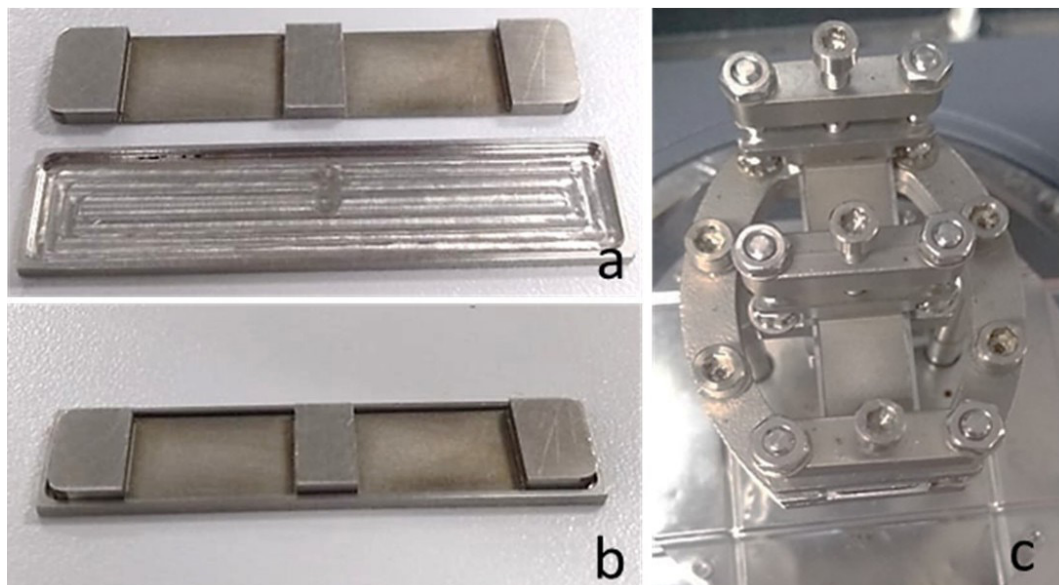
Figure 1. Powder sample holder, top plate, and open (a) and closed (b) bottom tray. Dual cantilever clamp with the powder holder.

with acetyl groups[22]. Furthermore, the elevated temperature increased the starch's swelling capacity and improved the diffusion rate of acetic anhydride[23].

After 20 minutes, the reaction temperature began to decline and remained constant until the end of the reaction. Upon reaching a maximum temperature of 70 °C, the reaction mixture transitioned from a cloudy white color to a transparent state, indicating a homogeneous distribution of reagents in the starch.

A high standard deviation in the DS was observed at the 90-minute mark. This variability likely resulted from secondary or parallel reactions that became more prominent with extended reaction times, leading to varying degrees of substitution across samples. Additionally, fluctuations in material homogeneity and temperature during the reaction likely contributed to this inconsistency. While longer reaction times may enhance reagent conversion, they also introduce complexities that undermine reproducibility and consistency.

The study by Sindhu et al.[24] explored the effects of acetylation on common buckwheat starch. According to the authors, prolonged reaction times tend to result in higher degrees of substitution, as extended exposure to the acetylating agent allows more acetyl groups to attach to the starch molecules. This observation aligns with the present study's findings, underscoring the importance of balancing

reaction time to optimize modification outcomes while maintaining consistency.

3.2. Determination of extent of acetylation by FTIR

Figure 3a presents FTIR spectra for samples collected at each reaction time, while Figure 3b highlights the band at 1740 cm^{-1}, corresponding to the carbonyl group of the acetyl group. The FTIR spectra confirmed the progression of acetylation during the reaction. Alongside the expected starch peaks, new peaks associated with acetyl groups emerged. The carbonyl band did not appear within the first 10 minutes of the reaction but became detectable after 20 minutes. Chemical determination of the DS revealed that acetylation had already commenced at 5 and 10 minutes, with DS values of 0.04 and 0.08, respectively. This discrepancy was attributed to the detection limits of FTIR, as low DS values may not produce sufficiently intense peaks to be detected. The sensitivity of FTIR strengthens this observation and provides a clearer interpretation of the results.

Figure 4 displays the extent of acetylation (EA) at each reaction time, alongside the DS values obtained via titration[25]. The EA was evaluated using the FTIR band ratio method, comparing the intensity of the acetyl C=O stretching band at 1740–1745 cm^{-1} with the C–O stretching intensity of the starch backbone at 1020–1040 cm^{-1} [26]. A direct comparison showed that the DS increased rapidly during the initial stages of the reaction, plateauing around 40 minutes, while the EA exhibited a more gradual rise before stabilizing after approximately 60 minutes.

This difference suggested that the incorporation of acetyl groups (DS) occurred predominantly during the early stages of the reaction, while the uniformity and distribution of these groups (EA) continued to improve over a longer duration. The relationship between EA and DS highlights a critical dynamic: while a high DS indicates significant chemical modification, EA provides insights into the homogeneity of substitution. A higher EA suggests a more uniform acetylation, which may enhance the functional properties of the modified starch, such as solubility or interaction with other components. Thus, understanding both metrics is
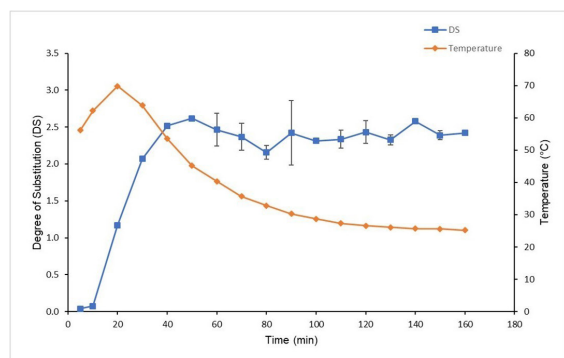
Figure 2. Degree of substitution (DS) and temperature graph for reaction time.

(a)   (b)
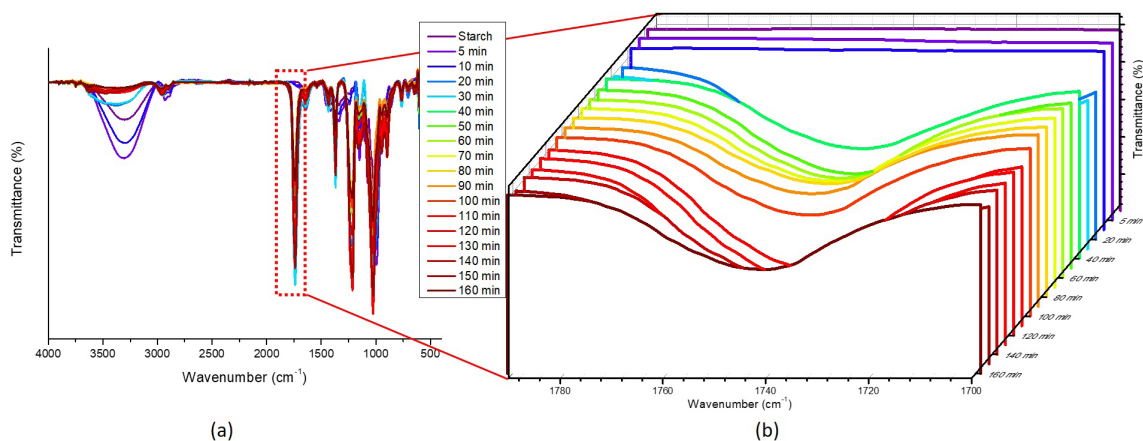
Figure 3. FTIR of samples at each reaction time (a) and band at 1740 cm^{-1} corresponding to stretching of carbonyl of acetyl group (b).

essential for optimizing reaction conditions to balance the degree and uniformity of substitution.

FTIR spectra for samples collected up to 50 minutes of reaction time, with a DS of 2.62, are presented in Figure 5. Five primary peaks were highlighted to demonstrate changes associated with acetylation. The O–H stretching band at 3284 cm^{-1} decreased in intensity as the DS increased, directly indicating the replacement of hydroxyl groups in starch with acetyl groups. Peaks associated with acetylation were observed at 1740 cm^{-1} (C=O stretching of carbonyl groups), 1373 cm^{-1} (C–H bending in –O(C=O)–CH$_3$), and 1221 cm^{-1} (C–O stretching of the acetyl group), confirming the successful modification of starch molecules[27].

Additionally, significant changes were observed in the disappearance of the 930 cm^{-1} peak, attributed to α1→4 glycosidic bond vibrations in amylose and amylopectin chains (Figure 6). This disappearance in samples with high DS suggested possible degradation of starch polymer chains during extended acetylation times. Previous studies on starch FTIR spectra have similarly reported structural changes detectable through shifts in comparable peaks, with slight variations in wave numbers[28].

3.3. Starch acetylation kinetics

Kinetic studies in solution were conducted to elucidate the reaction mechanism of starch acetylation, specifically to determine the rate law and rate constants. These studies confirmed pseudo-first-order kinetic behavior under the reaction conditions, consistent with previous findings on starch acetylation in similar systems[29,30]. Establishing this kinetic order enabled the calculation of reaction rates, reaction times, and optimal conditions for yield and efficiency. Integrated equations were applied to validate whether the concentration changes followed first-order kinetics, a characteristic frequently observed in acetylation reactions as reported in the literature[31].

The kinetic analysis was performed up to 40 minutes, as the DS increased significantly during this interval before reaching a plateau. This behavior suggested that most accessible hydroxyl groups reacted within this time frame, after which the reaction rate slowed considerably as it approached equilibrium. Limiting the kinetic study to this interval captured the primary active phase of acetylation,

where reaction dynamics were most pronounced, while data beyond 40 minutes contributed minimally to the kinetic understanding due to the stabilization of DS. Using Equations 4, 5 and 6, the data were plotted to derive the line equations and R^2 values for pseudo-first-order, second-order, and zero-order models, respectively.

Applying the integral analysis method, it was concluded that the starch acetylation reaction followed pseudo-first-order
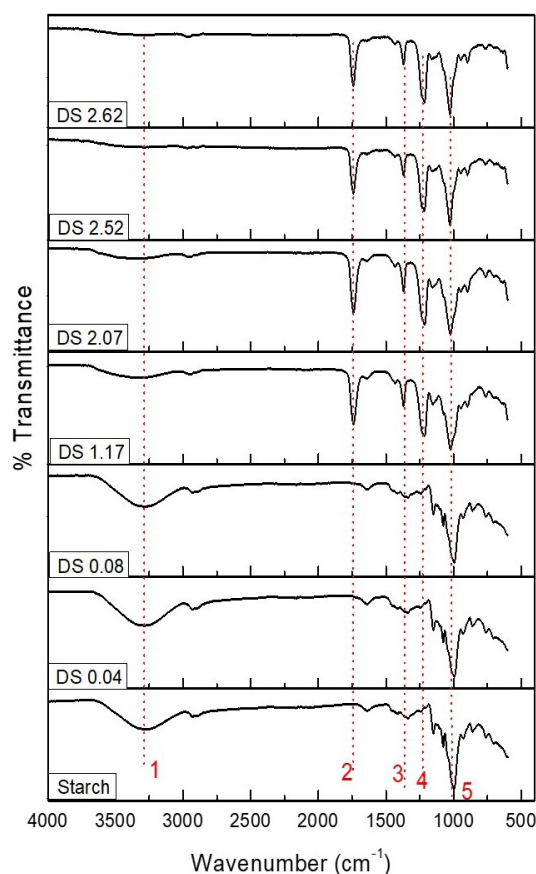
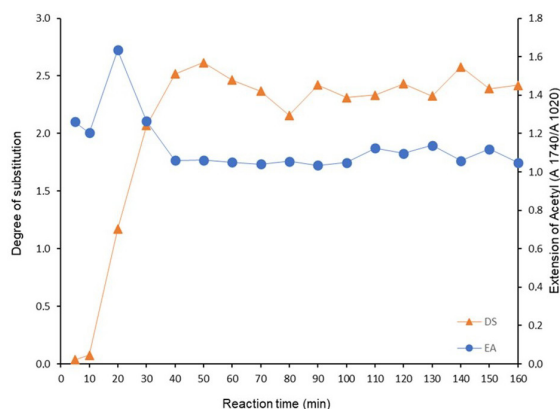**Figure 5.** FTIR of starch and acetylated starches with different DS.

Figure 4. Graph of extent of acetylation (EA) and degree of substitution (DS) for reaction time (min).
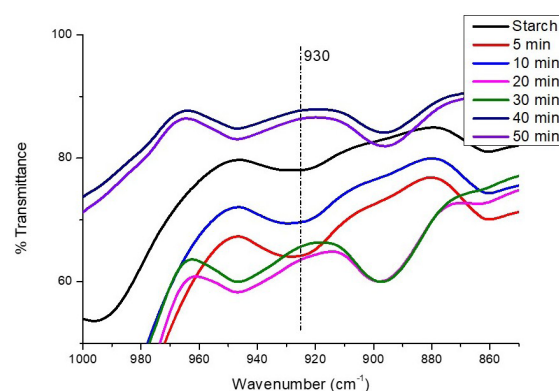
Figure 6. FTIR of starch and acetylated starches with different DS in wave number region at 930 cm^{-1}.

chemical kinetics. The pseudo-first-order curve (Figure 7a) exhibited the highest correlation coefficient (R^2), closest to 1, compared to the other models (Figures 7b and 7c). This result was expected since first-order reactions exhibit proportionality between the reaction rate and the concentration of reactants and products. This linearity was observed as the concentration of reactants (OH groups) decreased during the reaction. The angular coefficient, corresponding to the rate constant (k), was calculated using the integrated equation for pseudo-first-order kinetics, yielding a value of approximately 0.0609 s^{-1}.

Although the existing literature on starch acetylation predominantly focused on modifications in the properties

of acetylated starch and the various acetylation methods, a noticeable gap existed regarding the kinetics and thermodynamics of this reaction. Our findings, which revealed pseudo-first-order kinetics for corn starch acetylation, aligned with those reported for other substrates, such as corn cob[19] and wood[32]. These studies demonstrated similar reaction mechanisms, where the reaction rate was proportional to the concentration of hydroxyl groups, supporting the mechanism described in this work[33-36].

3.4. Thermodynamics of starch acetylation

The thermodynamic study of starch acetylation provided insights into the spontaneity, feasibility, and energetic requirements of the reaction. Key parameters, such as enthalpy (ΔH), entropy (ΔS), and heat capacity (Cp), were examined to assess the progression toward equilibrium and to understand the effects of temperature and reaction conditions on acetylation efficiency. These thermodynamic evaluations allowed for the optimization of reaction conditions by identifying the energetic favorability of acetyl group attachment to starch, consistent with findings in related acetylation[11,30].

Equation 7 enabled the plotting of $\ln \theta_T$ versus T^{-1}, where the slope of the line ($\Delta H/R$) and the Y-axis intercept ($\ln \theta$) provided $\ln \theta_0$, while the X-axis intercept (T^{-1}) yielded ΔH/RT_0. Here, ΔH represented the heat of starch acetylation, T_0 the critical temperature below which starch acetylation was not viable, and θ_0 the critical degree of starch acetylation. The equation of the line was expressed as $y=ax+b$, and Equation 10 below shows the line equation obtained from the plot based on Equation 7.

$$y = -0.0016x + 0.0223 \tag{10}$$

To obtain these data, it was assumed that starch acetylation occurred as a surface equilibrium reaction. Using the line equation, the heat of starch acetylation (ΔH) was calculated to be approximately -1.33×10^{-2} $J \cdot mol^{-1}$, confirming an exothermic reaction, as evidenced by the increase in temperature over the reaction time. The critical temperature (T_0) and critical degree of acetylation (θ_0) were determined to be 0.0223 K and 1.0226, respectively.

Heat capacity (Cp) for the starch acetylation reaction at constant pressure was calculated using Equation 8. Cp represented amount of heat required for starch acetylation as the temperature increased, with the variation ($T_2 - T_1$) represented this temperature change. Heat capacity obtained was 1.53×10^{-3} $J.mol^{-1}.K^{-1}$.

Using the C_p value, the entropy change of the acetylation reaction was determined with Equation 9. Since the reaction was conducted under constant pressure, the pressure variation value was zero. The entropy change (ΔS) calculated for starch acetylation was -2.31×10^{-4} $J \cdot mol^{-1} \cdot K^{-1}$. According to research by Nwadiogbu et al.[19], a very low critical temperature suggests that acetylation in the presence of a catalyst is a process that occurs spontaneously. However, the negative entropy value indicates the opposite.

As far as the literature indicates, no other studies have reported on the thermodynamics of starch acetylation, except for the work by Nwadiogbu et al.[19], which investigated the acetylation of corn cob. A comparison with the literature reveals notable differences in enthalpy, entropy, and heat capacity
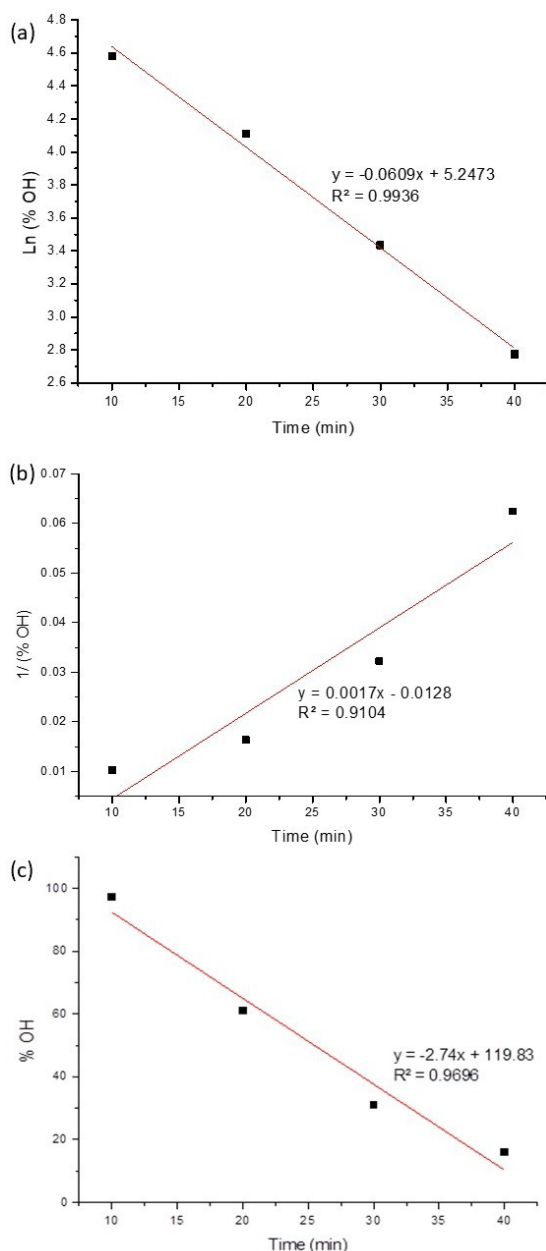
Figure 7. Rate curve of starch acetylation reaction - Order 1 (a); Order 2 (b) and Order 0 (c).

values, which can be attributed to variations in substrate composition and reaction conditions. The negative entropy value observed in this study contrasts with the positive entropy reported for corn cob acetylation, suggesting a lower degree of molecular disorder during starch acetylation. Furthermore, the differences in heat capacity reflect the varying thermal energy requirements between starch and corn cob systems

The entropy value (ΔS) is closely related to the spontaneity of the reaction. A negative ΔS reflects a low degree of disorder in the starch acetylation reaction. However, spontaneity is ultimately determined by the overall Gibbs free energy (ΔG), which considers both enthalpy (ΔH) and entropy (ΔS). In this case, the exothermic nature of the reaction (negative ΔH) drives the reaction forward, even in the presence of a negative ΔS. The catalyst played a critical role in overcoming the activation energy barrier, facilitating the reaction despite the unfavorable entropy change.

3.5. Scanning Electron Microscopy (SEM)

SEM analysis was performed to morphologically characterize starch granules before and after acetylation. Figure 8 presents micrographs of starch and starch acetates with DS values of 0.04, 0.08, 1.17, 2.07, 2.52, and 2.62 at different magnifications. Native corn starch granules exhibited irregularly shaped polygonal structures with smooth surfaces.

As the DS increased, SEM images revealed significant morphological changes in the starch granules. Larger pores began to form on the granule surfaces, likely due to the partial disruption of the granular structure caused by the incorporation of acetyl groups. This increase in porosity can be attributed to the chemical modification process, where the substitution of hydroxyl groups with bulky acetyl groups introduces steric hindrance and disrupts the hydrogen bonding network within the starch, rendering the structure more open and accessible[37].

In addition to increased porosity, SEM images also demonstrated the fusion of starch granules at higher DS levels. This phenomenon can be explained by the hydrophilic nature of the acetyl groups, which alter the surface properties of the granules. The agglomeration observed in the micrographs likely results from the formation of hydrogen bonds or other intermolecular forces between adjacent starch acetate molecules. These structural changes are significant, as they can influence the functional properties of starch acetates, including solubility, swelling behavior, and their suitability for various industrial applications[38].

Previous studies have reported similar changes in starch granules, including surface erosion, the formation of ditches and cavities, and a tendency for granule aggregation[25]. The introduction of bulky acetyl groups caused ruptures in the starch granules. Acetylation primarily occurred in the amorphous regions of the granules, composed of amylose, due to the limited penetration capacity of acetic anhydride in the crystalline lamellae of the granules. Nonetheless, during acetylation, the granules became more porous[39].

3.6. X-ray Diffraction (XRD)

The X-ray diffraction (XRD) technique was employed to examine changes in crystallinity resulting from starch acetylation. As shown in Figure 9a and Table 1, the degree

Table 1. Crystallinity index (%Xc) of native starch and starch acetates with different reaction times.

Sample	DS	%Xc
Starch	0	39.48
5 min	0.04	33.23
10 min	0.08	29.84
20 min	1.17	28.95
30 min	2.07	28.23
40 min	2.52	27.68
50 min	2.62	31.74

of crystallinity consistently decreased as the DS increased. Specifically, crystallinity dropped from 39.48% in native starch to 31.74% in the starch acetate with the highest DS. This decrease suggests that acetylation disrupts the crystalline structure of starch.

Corn starch crystallinity typically arises from double helices formed through intermolecular hydrogen bonding within amylopectin segments[40,41]. In agreement with the FTIR analysis, acetylation replaces some hydroxyl groups with acetyl groups, weakening both intermolecular and intramolecular hydrogen bonds. This substitution disrupts the organized crystalline structure of starch, partially breaking it down during acetylation.
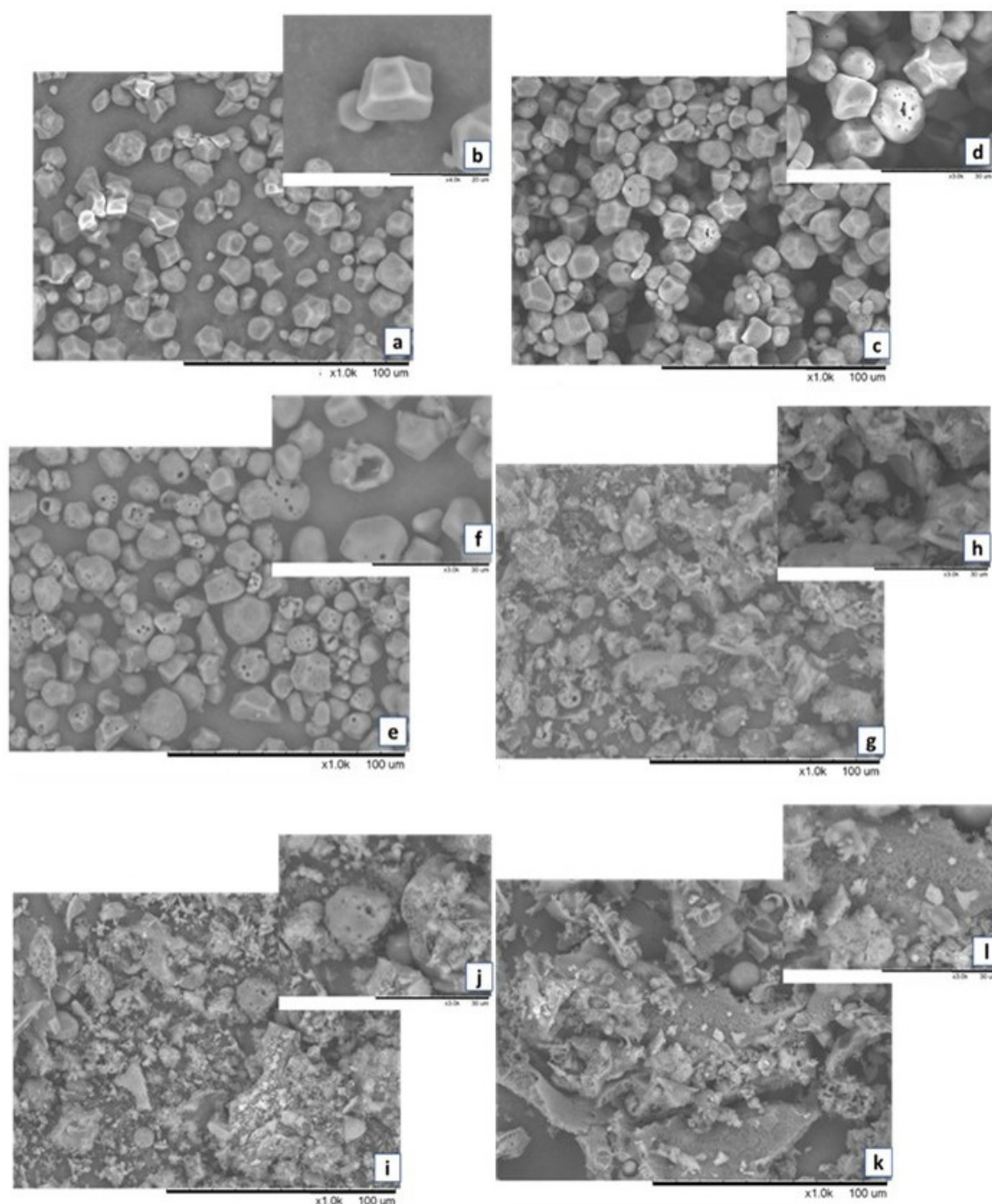
Starch and starch acetates with DS values of 0.04 and 0.08 displayed characteristic diffraction peaks of higher intensities at approximately $2\theta = 15°$, $17°$, $18°$, $20°$, and $23°$. These peaks are typical of starch with a monoclinic or type A crystalline structure, characterized by short amylopectin chains and dense branching, commonly found in cereal starches. In starch acetate with a DS of 1.17, the same peaks were present but exhibited reduced intensity.

For starch acetates with high DS values (2.07, 2.52, and 2.62), the type A crystalline structure was completely altered, and new broad peaks appeared at $2\theta = 9.5°$ and $20°$, indicating a structural transformation due to acetyl group incorporation. These findings are consistent with the results of Chi et al.[41], who also observed the disappearance of the native crystalline structure in corn starch upon acetylation. Both studies highlighted the emergence of a new crystalline pattern with characteristic peaks at 9° and 20° (2θ).

The broad peak and increased intensity at 20° (2θ) are attributed to type V starches, which form when acetylation increases the volume of the starch chains, making them more hydrophobic. Most starches are semicrystalline, with crystallinity ranging from 20% to 45%, depending on factors such as botanical origin, processing conditions, and the method used to determine the crystallinity index.

3.7. Dynamic Mechanical Analysis (DMA)

Dynamic Mechanical Analysis (DMA) is particularly effective for detecting changes in mechanical strength near the glass transition temperature (Tg), especially in self-supporting systems such as films or fibers. Although its application to powder samples is unconventional—powders are typically analyzed thermally using techniques like TGA or DSC—DMA's high sensitivity makes it a superior method for analyzing Tg in powders with low amorphous content.

Figure 8. SEM images of starch samples (a,b) and starch acetates: DS0.04 (c,d); DS0.08 (e,f); DS1.17 (g,h); DS2.07 (i,j) and DS2.52 (k,l) with different magnifications.

For this reason, DMA was employed to analyze starch and starch acetates with DS values of 0.08, 1.17, and 2.62[20,42].

Figure 9b shows the tan delta results for starch and starch acetates. The tan delta peaks decreased as the degree of acetylation increased, with highly acetylated starch (DS 2.62) exhibiting no detectable peaks. This reduction is attributed to the disruption of intra- and intermolecular hydrogen bonds in the amorphous regions by acetyl groups, which weakens

associative forces and stabilizing interactions. Consequently, fewer chain relaxations occur, as reflected by the diminishing tan delta peaks. The absence of a glass transition in highly acetylated starch suggests enhanced molecular mobility due to the disruption of its semi-crystalline nature[43].

Native starch displayed four peaks in the tan delta curve, likely corresponding to chain segment relaxations and amylopectin branch transitions. The peak at 141.6 °C
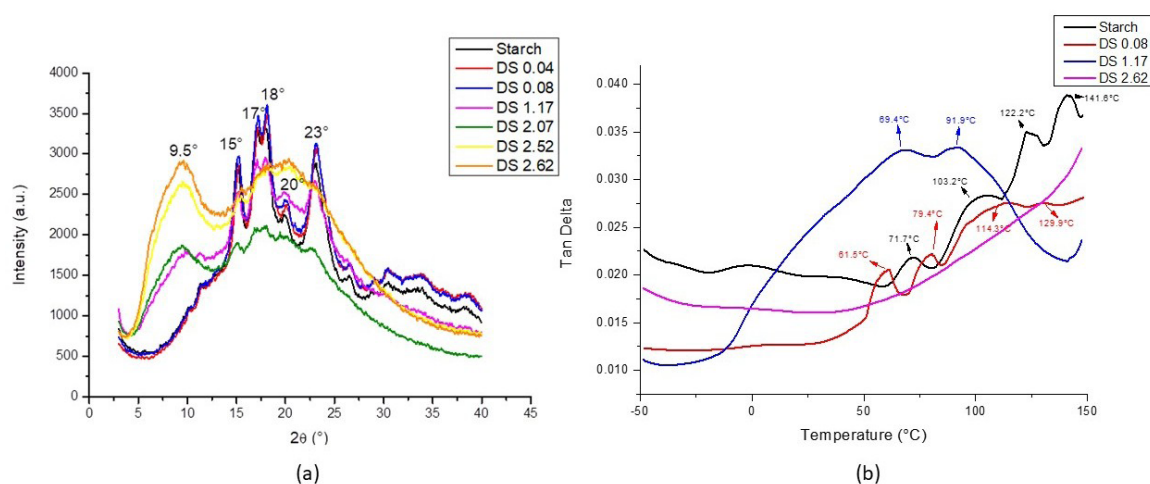
Figure 9. Diffractograms of starch and starch acetates with different DS (a) and Tan delta curves of powdered samples of starch and starch acetates with DS 0.08, 1.17, and 2.62 (b).

may indicate thermal degradation, as the starch exhibited a yellowish color characteristic of degradation after testing. The loss modulus is directly related to heat dissipation caused by the movement of long chain segments or side segment relaxations, such as those occurring during the glass transition. Acetylation appears to increase chain separation, making these relaxations more uniform. As a result, the peaks diminish, and highly acetylated starch exhibits no detectable transitions from the glassy to the rubbery state[44].

These findings align with previous studies. Garg and Kumar[45] reported greater thermal stability in acetylated starches with reduced hydroxyl groups, a conclusion supported by Rudnik et al.[46], who linked thermal stability to the reduction in hydroxyl groups. Similarly, Abedi et al.[29] demonstrated that starch acetylation, particularly when combined with sonication, improves thermal stability and reduces gelatinization enthalpy (ΔH), making starch more efficient in processes requiring thermal resistance.

FTIR, SEM, and XRD analyses confirm that acetylation introduces acetyl groups, increases porosity, and reduces crystallinity in starch, shifting its structure toward a more amorphous state with higher DS values. This structural modification is directly reflected in the DMA results, where the loss of crystallinity and hydrogen bonding leads to reduced tan delta peaks. The absence of a glass transition in highly acetylated starch (DS 2.62) indicates diminished chain interactions and greater molecular mobility, as acetyl groups disrupt the semi-crystalline structure of starch. Together, these findings suggest that acetylation not only modifies the molecular structure but also enhances the thermal stability and viscoelastic properties of starch, making it a promising material for applications requiring flexibility, thermal resistance, and durability.

The improved thermal stability and viscoelastic properties of acetylated starch expand its potential for industrial applications. For instance, these modifications make it suitable for biodegradable plastics, coatings, and adhesives, where enhanced flexibility and thermal resistance are critical. Additionally, the reduced gelatinization temperature and enthalpy increase its applicability in the food and pharmaceutical industries, where efficient processing and controlled functionality are essential[47].

4. Conclusion

This study investigated the kinetics and thermodynamics of starch acetylation and its influence on the properties of acetylated starches. The process was characterized as a surface reaction, where hydroxyl groups in corn starch were replaced by acetate groups, following pseudo-first-order kinetics with a high correlation coefficient (R^2 close to 1). Thermodynamic analysis indicated that the reaction was exothermic but non-spontaneous, requiring catalytic action to proceed efficiently.

A maximum DS of approximately 2.62 was achieved within 50 minutes, after which DS stabilized around 2.5 due to the equilibrium nature of the reaction, where deacetylation could occur under specific conditions. FTIR spectra confirmed successful acetylation by the appearance of a carbonyl band at ~1740 cm^{-1} and the disappearance of the peak at 930 cm^{-1}, suggesting some degradation of the starch polymer chains with prolonged reaction times.

X-ray diffraction and SEM analyses revealed that acetylation reduced the starch crystallinity from 39.48% to 31.74% and caused significant morphological changes, including granule disintegration and agglomeration. The reduction in tan delta peak intensity with higher DS reflected changes in relaxation behavior, with highly acetylated starch exhibiting no transition from a glassy to a rubbery state.

These structural and thermal modifications have significant implications for industrial applications. The reduced crystallinity and enhanced thermal stability make acetylated starch suitable for film formation in packaging, offering greater flexibility and reduced water sensitivity. Additionally, the changes in relaxation behavior and glass transition properties support its use in coatings and adhesives, where thermal stability is crucial. Furthermore, the improved properties imparted by acetylation enhance its performance in controlled-

release systems, making it valuable for agricultural and pharmaceutical applications. This study demonstrates that high DS in acetylated starch profoundly alters its structural, thermal, and mechanical properties, thus broadening its industrial potential.

5. Acknowledgments

6. References

1. Denardin CC, da Silva LP. Estrutura dos grânulos de amido e sua relação com propriedades físico-químicas. Cienc Rural. 2009;39(3):945-54. http://doi.org/10.1590/S0103-84782009005000003.

2. Carmo KP, Paiva JMF. Biodegradable films and starch compositions with other materials. Rev Virtual Quim. 2015;7(6):2377-86. http://doi.org/10.5935/1984-6835.20150141.

3. Khan Z, Javed F, Shamair Z, Hafeez A, Fazal T, Aslam A, et al. Current developments in esterification reaction: a review on process and parameters. J Ind Eng Chem. 2021;103:80-101. http://doi.org/10.1016/j.jiec.2021.07.018.

4. Larotonda FDS, Matsui KN, Soldi V, Laurindo JB. Biodegradable films made from raw and acetylated cassava starch. Braz Arch Biol Technol. 2004;47(July):477-84. http://doi.org/10.1590/S1516-89132004000300019.

5. Trela VD, Ramallo AL, Albani OA. Synthesis and characterization of acetylated cassava starch with different degrees of substitution. Braz Arch Biol Technol. 2020;63:e20180292. http://doi.org/10.1590/1678-4324-2020180292.

6. Lin D, Zhou W, Zhao J, Lan W, Chen R, Li Y, et al. Study on the synthesis and physicochemical properties of starch acetate with low substitution under microwave assistance. Int J Biol Macromol. 2017;103:316-26. http://doi.org/10.1016/j.ijbiomac.2017.05.056.

7. Muljana H, Picchioni F, Knez Z, Heeres HJ, Janssen LPBM. Insights in starch acetylation in sub- and supercritical CO2. Carbohydr Res. 2011;346(10):1224-31. http://doi.org/10.1016/j.carres.2011.04.002.

8. Xiao H, Yang T, Lin Q, Liu GQ, Zhang L, Yu F, et al. Acetylated starch nanocrystals: preparation and antitumor drug delivery study. Int J Biol Macromol. 2016;89:456-64. http://doi.org/10.1016/j.ijbiomac.2016.04.037.

9. Tuovinen LM, Peltonen SH, Suortti TM, Crowther NJ, Elomaa MA, Järvinen KP. Enzymatic degradation of and bovine serum albumin release from starch-acetate films. Biomacromolecules. 2002;3(2):284-90. http://doi.org/10.1021/bm015581e.

10. Betancur AD, Chel GC, Cañizares HE. Acetylation and characterization of canavalia ensiformis starch. J Agric Food Chem. 1997;45(2):378-82. http://doi.org/10.1021/jf960272e.

11. Wang YJ, Wang L. Characterization of acetylated waxy maize starches prepared under catalysis by different alkali and alkaline-earth hydroxides. Stärke. 2002;54(1):25-30. http://doi.org/10.1002/1521-379X(200201)54:1<25::AID-STAR25>3.0.CO;2-T.

12. Kim HS, Choi HS, Kim BY, Baik MY. Characterization of acetylated corn starch prepared under ultrahigh pressure (UHP). J Agric Food Chem. 2010;58(6):3573-9. http://doi.org/10.1021/jf903939y.

13. Biswas A, Shogren RL, Willett JL. Solvent-free process to esterify polysaccharides. Biomacromolecules. 2005;6(4):1843-5. http://doi.org/10.1021/bm0501757.

14. Pu H, Chen L, Li X, Xie F, Yu L, Li L. An oral colon-targeting controlled release system based on resistant starch acetate: synthetization, characterization, and preparation of film-coating pellets. J Agric Food Chem. 2011;59(10):5738-45. http://doi.org/10.1021/jf2005468.

15. De Graaf RA, Broekroelofs GA, Janssen LPBM, Beenackers AACM. The kinetics of the acetylation of gelatin&d potato starch. Carbohydr Polym. 1995;28(95):137-44. http://doi.org/10.1016/0144-8617(95)00088-7.

16. Li J, Wang H, Wang X, Jiang L, Su X, Fang K, et al. A synthesis of irradiated and vinyl acetate esterified starch accompanied with microstructural and macroscopic property analysis. Mater Today Commun. 2024;41:110437. http://doi.org/10.1016/j.mtcomm.2024.110437.

17. Lin J, Li E, Li C. Increasing degree of substitution inhibits acetate while promotes butyrate production during in vitro fermentation of citric acid-modified rice starch. Int J Biol Macromol. 2024;281:136385. http://doi.org/10.1016/j.ijbiomac.2024.136385.

18. Chen B, Jin G, Ji S, Qiao D, Zhao S, Zhang B. Acetated starch inclusion to tailor the hierarchical structure and sol-gel features of middle gluten wheat starch-based binary matrices. Food Hydrocoll. 2025;160:110764. http://doi.org/10.1016/j.foodhyd.2024.110764.

19. Nwadiogbu JO, Okoye PAC, Ajiwe VI, Nnaji NJN. Hydrophobic treatment of corn cob by acetylation: kinetics and thermodynamics studies. J Environ Chem Eng. 2014;2(3):1699-704. http://doi.org/10.1016/j.jece.2014.06.003.

20. Mahlin D, Wood J, Hawkins N, Mahey J, Royall PG. A novel powder sample holder for the determination of glass transition temperatures by DMA. Int J Pharm. 2009;371(1–2):120-5. http://doi.org/10.1016/j.ijpharm.2008.12.039.

21. Colussi R, El Halal SLM, Pinto VZ, Bartz J, Gutkoski LC, Zavareze ER, et al. Acetylation of rice starch in an aqueous medium for use in food. Lebensm Wiss Technol. 2015;62(2):1076-82. http://doi.org/10.1016/j.lwt.2015.01.053.

22. Volkert B, Lehmann A, Greco T, Nejad MH. A comparison of different synthesis routes for starch acetates and the resulting mechanical properties. Carbohydr Polym. 2010;79(3):571-7. http://doi.org/10.1016/j.carbpol.2009.09.005.

23. Tupa MV, Ávila Ramírez JA, Vázquez A, Foresti ML. Organocatalytic acetylation of starch: effect of reaction conditions on DS and characterisation of esterified granules. Food Chem. 2015;170:295-302. http://doi.org/10.1016/j.foodchem.2014.08.062.

24. Sindhu R, Devi A, Khatkar BS. Morphology, structure and functionality of acetylated, oxidized and heat moisture treated amaranth starches. Food Hydrocoll. 2021;118:106800. http://doi.org/10.1016/j.foodhyd.2021.106800.

25. Golachowski A, Zięba T, Kapelko-Żeberska M, Drożdż W, Gryszkin A, Grzechac M. Current research addressing starch acetylation. Food Chem. 2015;176:350-6. http://doi.org/10.1016/j.foodchem.2014.12.060.

26. Adebajo MO, Frost RL, Kloprogge JT, Kokot S. Raman spectroscopic investigation of acetylation of raw cotton. Spectrochim Acta A Mol Biomol Spectrosc. 2006;64(2):448-53. http://doi.org/10.1016/j.saa.2005.07.045.

27. Xu Y, Miladinov V, Hanna MA. Synthesis and characterization of starch acetates with high substitution. Cereal Chem. 2004;81(6):735-40. http://doi.org/10.1094/CCHEM.2004.81.6.735.

28. Dankar I, Haddarah A, Omar FEL, Pujolà M, Sepulcre F. Characterization of food additive-potato starch complexes by FTIR and X-ray diffraction. Food Chem. 2018;260:7-12. http://doi.org/10.1016/j.foodchem.2018.03.138.

29. Abedi E, Roohi R, Hashemi SMB, Kaveh S. Investigation of ultrasound-assisted starch acetylation by single- and dual-frequency ultrasound based on rheology modelling, non-isothermal reaction kinetics, and flow/acoustic simulation. Ultrason Sonochem. 2024;102:106737. http://doi.org/10.1016/j.ultsonch.2023.106737.

30. Kumoro AC, Amalia R. Mass transfer and chemical reaction approach of the kinetics of the acetylation of gadung flour using glacial acetic acid. Bull Chem React Eng Catal. 2015;10(1):30-7. http://doi.org/10.9767/bcrec.10.1.7181.30-37.

31. Oliveira AP, Faria RB. Ordens não inteiras em cinética química. Quim Nova. 2010;33(6):1412-5. http://doi.org/10.1590/S0100-40422010000600035.

32. Hill CAS, Jones D, Strickland G, Cetin NS. Kinetic and mechanistic aspects of the acetylation of wood with acetic anhydride. Holzforschung. 1998;52(6):623-9. http://doi.org/10.1515/hfsg.1998.52.6.623.

33. Chi C, Lian S, Zou Y, Chen B, He Y, Zheng M, et al. Preparation, multi-scale structures, and functionalities of acetylated starch: an updated review. Int J Biol Macromol. 2023;249:126142. http://doi.org/10.1016/j.ijbiomac.2023.126142.

34. Cao C, Wang C, Yuan D, Kong B, Sun F, Liu Q. Effects of acetylated cassava starch on the physical and rheological properties of multicomponent protein emulsions. Int J Biol Macromol. 2021;183:1459-74. http://doi.org/10.1016/j.ijbiomac.2021.05.134.

35. Ge X, Hu Y, Shen H, Liang W, Sun Z, Zhang X, et al. Electron beam irradiation application for improving the multiscale structure and enhancing physicochemical and digestive properties of acetylated naked barley. Food Chem. 2023;404:134674. http://doi.org/10.1016/j.foodchem.2022.134674.

36. Kaushik R, Kumar A, Rani N, Phogat R, Gehlot R. Acetylation/esterification of starch. Boca Raton: CRC Press; 2024. Starch: structure, properties, and modifications for food applications; p. 281-313. http://doi.org/10.1201/9781032655598-12

37. Singh B, Chauhan GS, Kumar S, Chauhan N. Synthesis, characterization and swelling responses of pH sensitive psyllium and polyacrylamide based hydrogels for the use in drug delivery (I). Carbohydr Polym. 2007;67(2):190-200. http://doi.org/10.1016/j.carbpol.2006.05.006.

38. Wawrzkiewicz M, Podkościelna B, Tarasiuk B. Modified starch as a component of environmentally friendly polymer adsorbents: from synthesis and characterization to potential application in the removal of toxic C.I. Basic Yellow 2 dye. Measurement. 2025;240:115556. http://doi.org/10.1016/j.measurement.2024.115556.

39. Diop CIK, Li HL, Xie BJ, Shi J. Effects of acetic acid/acetic anhydride ratios on the properties of corn starch acetates. Food Chem. 2011;126(4):1662-9. http://doi.org/10.1016/j.foodchem.2010.12.050.

40. Punia S. Barley starch modifications: Physical, chemical and enzymatic - A review. Int J Biol Macromol. 2020;144:578-85. http://doi.org/10.1016/j.ijbiomac.2019.12.088.

41. Chi H, Xu K, Wu X, Chen Q, Xue D, Song C, et al. Effect of acetylation on the properties of corn starch. Food Chem. 2008;106(3):923-8. http://doi.org/10.1016/j.foodchem.2007.07.002.

42. McPhillips H, Craig DQM, Royall PG, Hill VL. Characterisation of the glass transition of HPMC using modulated temperature differential scanning calorimetry. Int J Pharm. 1999;180(1):83-90. http://doi.org/10.1016/S0378-5173(98)00407-4.

43. Lee HL, Yoo B. Dynamic rheological and thermal properties of acetylated sweet potato starch. Stärke. 2009;61(7):407-13. http://doi.org/10.1002/star.200800109.

44. Cassu SN, Felisberti MI. Dynamic mechanical behavior and relaxations in polymers and polymeric blends. Quim Nova. 2005;28(2):255-63. http://doi.org/10.1590/S0100-40422005000200017.

45. Garg S, Jana AK. Characterization and evaluation of acylated starch with different acyl groups and degrees of substitution. Carbohydr Polym. 2011;83(4):1623-30. http://doi.org/10.1016/j.carbpol.2010.10.015.

46. Rudnik E, Matuschek G, Milanov N, Kettrup A. Thermal properties of starch succinates. Thermochim Acta. 2005;427(1-2):163-6. http://doi.org/10.1016/j.tca.2004.09.006.

47. Subroto E, Cahyana Y, Indiarto R, Rahmah TA. Modification of starches and flours by acetylation and its dual modifications: a review of impact on physicochemical properties and their applications. Polymers (Basel). 2023;15(14):2990. http://doi.org/10.3390/polym15142990.